Computational investigation of phytochemicals from Allamanda cathartica as a potent agonist of Peroxisome proliferator-activated receptor-gamma (PPARγ) for the treatment of Diabetes mellitus

Ritu Tomar
Dehradun Institute of Technology University
Shashank Mishra
Dehradun Institute of Technology University
Jagannath Sahoo
NMIMS University
Santosh Kumar Rath
skrath1985@gmail.com

Dehradun Institute of Technology University

Research Article

Keywords: Molecular docking, Allamanda cathartica, PPARγ agonist, Molecular dynamic simulation, Diabetes.

Posted Date: April 9th, 2024

DOI: https://doi.org/10.21203/rs.3.rs-4214253/v1

Additional Declarations: No competing interests reported.

Abstract

Diabetes, a chronic metabolic disease, has become a serious health problem worldwide. According to the latest data from the International Diabetes Federation (IDF), there were 451 million DM patients worldwide in 2017, and would be expected to increase to 693 million by 2045. Therefore, there is a need to develop new drug-like molecules to combat this problem. Peroxisome proliferators-activated receptors (PPARs) are ligand-inducible nuclear receptors that control many intracellular metabolic processes. PPARγ agonists can improve metabolism and reduce the side effects caused by single drugs and have become a valuable drug target for designing effective drugs for the treatment of type 2 diabetes. In the present investigation, by the application of bioactivity score prediction, molecular docking, and ADMET prediction approach, the potential and selective phytoconstituents with the highest binding affinity, and lower toxicity than reference drug rosiglitazone was gained from the curated datasets of *Allamanda cathartica*. Further molecular dynamics simulations were carried out to identify the favourable binding conformations when the top-scored phytoconstituents bind with the PPARγ receptors compared to the rosiglitazone. Compound **AC2** interacts with the PPARγ proteins through the formation of 7 hydrogen bonds with the amino acid residues Phe282, His449, Tyr327, His323 and Ser289. The ligand was bound to the protein during the simulation since none of the complexes conformations were unstable and no unfolding or folding took place. Our results provided an approach to further design and optimize the natural product-inspired small druglike molecules as potential antidiabetic agents. The present study highlighted that the phytoconstituents of *Allamanda cathartica* has antidiabetic potential as PPARγ agonists that can be further explored for novel antidiabetic drug development.

1. Introduction

More than 400 million people worldwide have been affected by diabetes mellitus (DM), a serious public health problem (Jain & Laiteerapong, 2015). This metabolic condition develops chronic, life-threatening microvascular, macrovascular, and neuropathic consequences over time. Diabetes mellitus (DM) is brought on by a lack of insulin production, pancreatic cell injury, or insulin resistance brought on by inadequate insulin use. The trend towards sedentary living may be the main cause of the rising number of diabetic patients worldwide, which is predicted to reach 366 million in the older population (>65 years) by 2030 (McIntyre et al., 2019; Kurtzhals et al., 2018). Nephropathy, neuropathy, cardiovascular and renal issues, retinopathy, food-related diseases, and more are among the many consequences linked to DM. The two varieties of DM are type 1 and type 2. The management of metabolic syndrome (MS) and type 2 diabetic mellitus (T2DM) puts a significant emphasis on the creation of novel PPAR agonists (Unnikrishnan, Anjana & Mohan, 2016). Pharmacological drugs that target PPARs fall into at least two different types. The fibrates are PPAR ligands, which are employed. Thiazolidinediones (TZDs), including rosiglitazone and pioglitazone, are PPAR full agonists used as insulin sensitizers in the treatment of type 2 diabetes. TZDs are also utilised for the control of hypercholesterolemia. Rosiglitazone was reported to have significant side effects, including fluid retention, weight gain, and an increased risk of a cardiovascular event, despite its obvious efficacy in lowering blood sugar levels (Hong et al., 2018; Yun,

Han, & Park, 2018). These side effects prompted some regulatory organisations across the globe to limit or halt the use of rosiglitazone (Engwa et al., 2018;). Pioglitazone was found to be a safer drug than rosiglitazone, presenting two intriguing questions about how the two medications interact (Bermúdez et al., 2010; Mudaliar & Henry, 2004). Small differences in the binding manner, such as those seen between rosiglitazone and pioglitazone, can have a significant impact on the pharmacological profile, including the adverse effects, as mentioned by Bruning and colleagues (Bruning et al., 2007). The activation of PPAR by fibrates, another class of PPAR agonists, is well recognised to lower triglyceride levels and raise HDL levels (both of which are significant precursors to the development of T2DM) (Shi, Zhao, & Qi, 2018). The anti-obesity and anti-inflammatory properties of PPAR (the less studied of the PPARs) have been linked to conditions like arthritis, eczema, and psoriasis, supporting the receptor's potential benefits in the treatment of chronic and metabolic disorders (Jia et al., 2018; Liu et al., 2018; Cheng et al.,

2014). It is unknown whether the majority of PPAR dual- and pan-agonists created to date can truly exhibit *in vivo* therapeutic effects due to the clinical studies being stopped due to the negative effects seen in these tests.

In tropical and subtropical areas of the world, *Allamanda cathartica* is a perennial, half-hardy evergreen woody shrub that resembles a vine, compact or creeping, decorative, or garden flowering plant. It is a member of the *Apocynaceae* family and is native to Brazil, as well as India and Sri Lanka (Petricevich & Abarca-Vargas, 2019). It is referred to as "Malatilata," "Pilaghanti," and "Harkakra" in India. In addition to being a good purgative, this plant also functions as an antidote for poisoning and treats inflammation, constipation, ascites, sores, and ulcers (Bonomini et al., 2017). In ascites, the bark functions as a hydragogue, and in small dosages, the leaves are an effective cathartic. For snake bites, the root is used as a treatment. The entire plant is used to treat skin burns. It is effective against jaundice, malaria, and fungal infections, as well as having antithrombotic, immunomodulatory, cardiovascular, anti-ischemic, antiarrhythmic, antiangiogenic, antimutagenic, and gastroprotective properties (Prabhadevi et al., 2012; Rodrigues et al., 2020; Dokhe et al., 2023). Long-chain esters, triterpene esters, isoplumericin, plumericin, and plumeride are found in the roots. In contrast, hydrocarbons, long-chain esters, isoplumericin, plumericin, and plumeride, as well as ursolic acid, are present in the leaves. There have been seven identified compounds from this species (Petricevich & Abarca-Vargas, 2019). The existence of antileukemic iridoids and lactones from *Allamanda cathertica* has demonstrated the species' anticancer efficacy. This plant is chosen to isolate bioactive anticancer chemicals because of this.

In this research investigation, we performed bioactivity score analysis to evaluate the therapeutic potential of the phytoconstituents of *Allamanda cathertica*. Further molecular docking was performed to find selective and potential lead compounds targeting PPARγ. The retrieved best phytoconstituents were applied to ADMET prediction. Subsequently, a compound with the highest docking score, good binding interactions, lowest toxicity and druggability was subjected to molecular dynamics simulations (MDs) to identify potential PPARγ agonists. We hope the findings obtained from this investigation will help in the search for potential and selective phytoconstituents as PPARγ agonists by identifying the structural features involved in the binding process.

2. Materials & methods

2.1 Selection of phytoconstituents

A curated dataset of 39 phytoconstituents of *Allamanda cathertica* was selected for the studies (Hameed, Nawaz & Gulzar, 2014). The structures of the following active compounds of *A. cathertica* were drawn in the molecule editor and saved in SDF format. The energy of the compounds was optimized by using the MMFF94 force field. The structures of the selected compounds are given in Figs. 1 & 2.

2.2 Bioactivity score prediction

The diversity of possible drug targets (of which each requires a different combination of matching molecular characteristics) is so enormous, that it is possible to find a common denominator for all of them and to express molecule drug-likeness by a single "magic number". Simple count criteria (like limits for molecular weight, log P, or number of hydrogen bond donors or acceptors) have also relatively limited applicability and are useful only to discard obvious non-drugs (Shekhar et al., 2016). The strategy which leads to success is not a universal drug-likeness score, but a focus on particular drug classes and the development of specific activity scores for each of these classes. The method we implemented uses sophisticated Bayesian statistics to compare structures of representative ligands active on the particular target with structures of inactive molecules and to identify substructure features (which in turn determine physicochemical properties) typical for active molecules (Sharma et al., 2016). The bioactivity of all selected phytoconstituents was evaluated against six different protein structures by using the tool Molinspiration Cheminformatics server (http://www.molinspiration.com).

2.3 Molecular docking analysis

To explore the antidiabetic potential of the *Allamanda cathertica* we selected three proteins to know how the phytoconstituents of *Allamanda cathertica* exert the antidiabetic effects. The crystal structures of dipeptidyl peptidase IV in complex with TAK-322 (PDB ID: 3G0B), Structure of the human GLP-1 receptor complex with NNC0640 (PDB ID: 5VEX) and Human PPARgamma ligand binding domain complexed with Rosiglitazone (PDB ID: 5YCP) were downloaded from RCSB Protein Data Bank (PDB, www.pdb.org) (Cronet et al., 2001; Nolte et al., 1998). The LigandScout program advanced version was used to perform binding affinity prediction of the phytoconstituents for three different proteins. All the retrieved proteins were pre-processed by including the missing hydrogen atoms and optimizing energy. The co-crystallized ligands were present, therefore binding pocket was selected as a grid for the docking. Only the binding sites were covered by this docking grid, not the target's whole surface. The AutoDock 4.2 program was utilized to dock the ligands, and its default parameters of 20 genetic algorithms run, 2.0 Å RMSD cluster tolerance, 2500000 energy evaluations, and 27000 max. number of generations were used. Furthermore, the anticipated binding energy (ΔG, Kcal/mol) is used by Autodock docking algorithms to score and rank the docked positions. The calculation of the binding energy for the ideal placements and the

visualisation of the interaction details were done with the help of the academic Maestro visualizer programme.

2.4 ADMET calculation

The property of ADMET refers to the absorption, distribution, metabolism, excretion, and toxicity. ADMET prediction of top-scored compounds was performed by using the pkCSM online tool for reducing waste of money and time in later drug development process. The pkCSM signatures were successfully used across five main pharmacokinetic properties classes to develop predictive regression and classification models (Pires, Blundell & Ascher, 2015).

2.5 Molecular dynamics simulation

Following the ADMET and molecular docking analysis, the top-scoring complexes were subjected to molecular dynamics simulations to determine their stability and validate the docking outcomes using the Desmond tool of Schrodinger (Sharma et al., 2023, Rath et al. 2019). Molecular dynamics (MD) is one of the most common methods in molecular modelling. This method is based on the molecular force field and can dynamically describe the movement of molecules and then describe the dynamic process of life (Feng et al., 2020, Dwibedi et al. 2023). PPARγ-**AC2** (1-deoxy-d-mannitol) and PPARγ-**AC31** (Phytol) complexes were selected for validation of docking outcomes. Both complexes were built in the simple point charge (SPC) water model and the system was prepared using a POPC membrane. The orthorhombic box was selected with the size of 10×10×10 Å. The salt concentration was set at 0.15 M to keep physiological conditions. The model systems were generated using the OPLS_2005 force field and neutralized by replacing solvent molecules with Na^+ or Cl^- ions. Further, model systems were relaxed before simulations using the hybrid method steepest decent and the limited-memory Broyden–Fletcher–Goldfarb–Shanno (LBFGS) algorithms for 2000 iterations. The complex system needs to be equilibrated with normal pressure and temperature (NPT) at a temperature of 300 K and normal pressure (1.01325 bar). A Nose-Hoover chain thermostat operating at 1 bar of pressure for 100 ns at constant temperature in conjunction with an isobaric isothermal ensemble (NPT equilibrium) was used to complete the simulation. After the simulation, all results were analyzed and saved for further research. The RMSD (root mean square deviation) and RMSF (root mean square fluctuation) of protein and protein-ligands complexes were analyzed and monitored at all times during MD simulations.

3. Results & discussions

3.1 Bioactivity score calculations

The bioactivity of all selected phytoconstituents was evaluated against six different protein structures. Biological activity is predicted by bioactivity scores that are categorized under three different ranges (Mishra et al., 2018).

- If the bioactivity score is more than 0.00, having considerable biological activity.

- If bioactivity score is 0.5 to 0.00, having moderate activity.
- If the bioactivity score is less than − 0.50, having inactivity.

The results of bioactivity score prediction are given in Table 1. Bioactivity score prediction results revealed that the majority of phytoconstituents are biologically active and have physiological effects. AC1, AC12, AC17, AC20, AC21 etc have activity scores against GPCR ligand and nuclear receptor ligand which indicates they could bind more effectively with GPCR and nuclear receptors. The bioactivity score provides information about the a binding cascade of the compounds that are used for the development of a new functional drug with increased binding selectivity profile and less undesirable effects (Sharma et al., 2016).

Table 1
Bioactivity score analysis of phytoconstituents of *Allamanda cathertica*

S. No.	Compounds	GPCR ligand	Ion channel modulator	Kinase inhibitor	Nuclear receptor ligand	Protease inhibitor	Enzyme inhibitor
1.	AC1	0.13	0.10	-0.31	0.89	0.05	0.78
2.	AC2	-0.90	-0.35	-1.08	-1.11	-0.99	-0.07
3.	AC3	-0.45	-0.08	-0.36	-0.23	-0.70	-0.11
4.	AC4	0.11	0.16	-0.32	0.35	0.00	0.31
5.	AC5	-0.63	-0.15	-0.85	-0.66	-0.35	0.20
6.	AC6	-0.58	-0.47	-0.19	-1.62	-0.83	-0.21
7.	AC7	0.33	0.23	-0.19	0.35	0.13	0.42
8.	AC8	0.29	0.17	-0.16	0.31	0.12	0.38
9.	AC9	-0.34	-0.24	-0.81	-0.48	-0.43	0.07
10.	AC10	0.20	0.03	-0.43	0.11	-0.01	0.21
11.	AC11	-0.24	-0.16	-0.77	0.15	-0.33	0.21
12.	AC12	0.04	-0.03	-0.45	0.19	-0.06	0.61
13.	AC13	-2.21	-1.57	-2.49	-2.05	-2.31	-1.60
14.	AC14	0.22	-0.05	-0.31	0.67	0.11	0.56
15.	AC15	-0.59	-0.18	-1.13	-1.69	-0.74	0.20
16.	AC16	0.07	-0.02	-0.30	0.29	0.13	0.20
17.	AC17	0.17	0.46	-0.34	0.05	0..07	0.45
18.	AC18	-0.30	0.00	-0.64	-0.95	-0.44	0.36
19.	AC19	-0.27	-0.04	-0.75	-0.24	-0.36	0.04
20.	AC20	0.19	-0.07	0.08	0.83	0.09	0.50
21.	AC21	0.02	0.06	-0.33	0.08	-0.04	0.18
22.	AC22	0.14	0.07	-0.45	0.16	-0.22	0.26
23.	AC23	-0.10	-0.21	0.21	0.32	-0.27	0.26
24.	AC24	0.27	0.11	-0.42	0.85	0.15	0.52
25.	AC25	0.03	-0.20	-0.26	0.42	-0.12	0.21
26.	AC26	0.14	0.05	-0.16	0.21	0.10	0.19

S. No.	Compounds	GPCR ligand	Ion channel modulator	Kinase inhibitor	Nuclear receptor ligand	Protease inhibitor	Enzyme inhibitor
27.	AC27	0.11	0.05	-0.20	0.17	0.06	0.20
28.	AC28	-0.68	-0.29	-1.38	-0.69	-0.79	-0.21
29.	AC29	0.17	0.07	-0.22	0.23	0.07	0.27
30.	AC30	-0.04	0.05	-0.42	0.01	-0.11	0.16
31.	AC31	0.11	0.16	-0.32	0.35	0.00	0.31
32.	AC32	0.14	0.07	-0.45	0.16	-0.22	0.26
33.	AC33	-0.08	-0.54	-0.48	-0.10	-0.00	0.02
34.	AC34	-0.02	-0.07	0.26	0.39	-0.22	0.28
35.	AC35	0.04	0.01	-0.10	0.19	-0.03	0.16
36.	AC36	-0.11	0.03	-0.51	-0.06	-0.19	0.13
37.	AC37	-2.60	-2.34	-2.81	-3.05	-3.15	-1.62
38.	AC38	0.28	-0.03	-0.50	0.89	0.23	0.69
39.	AC39	0.25	0.14	-0.21	0.41	0.28	0.24

3.2 Molecular docking analysis

To better understand the binding mechanism of the phytoconstituents with different 3 proteins molecular docking analysis was performed. The names and docking scores of these phytoconstituents are listed in Table 2. Docking results revealed that the majority of phytoconstituents show excellent binding for PPAR- γ protein. Compounds **AC6** (6,7-dimethylthieno (2,3-b) quinolin-3-ylamine), **AC14** (beta amyrin), **AC23** (kaempferol), and **AC33** (plumeride coumerate) exhibit the highest binding affinity for DPP-4 target protein while compound **AC16** (beta-sitosterol), **AC28** (octanoic acid) and **AC38** (ursolic acid) show better binding affinity for GLP-1 target protein.

Table 2

Docking scores of the phytoconstituents of *Allamanda cathertica* for PPAR- γ, GLP-1 and DPP-4 proteins

Compounds code	Compounds name	Docking score		
		PPAR-γ	GLP-1	DPP-4
AC1	1,2,3,4,4a,4b,5,6,7,8,8a,9-dodecahydro-7-hydroxy-2,4b,8,8-tetramethyl, 2-phenanthrenecarboxaldehyde	**-4.33**	-2.6	-3.16
AC2	1-deoxy-d-mannitol	**-7.39**	-6.96	-5.09
AC3	2-phenanthrenecarboxaldehyde	**-7.09**	-2.10	-4.20
AC4	3,7,11,15-tetramethyl-2-hexadecen-1-ol	**-7.03**	-0.04	-2.09
AC5	3-O-methyl-dglucose	**-6.85**	-6.09	-5.34
AC6	6,7-dimethylthieno (2,3-b) quinolin-3-ylamine	-3.67	-3.87	**-5.39**
AC7	9,12,15-octadecatrienoic acid,(Z,Z,Z)	**-5.91**	-2.50	-3.22
AC8	9,12-octadecadienoic acid,(linolic acid)	**-6.89**	-1.69	-2.76
AC9	11-oxatetracyclo[4.2.1.1(2,5).1(7,10)]undec-3-ene,9-methoxy-9-methyl-	**-3.16**	-1.53	-1.54
AC10	allamandicine	**-5.48**	-2.44	-5.14
AC11	allamandin	**-3.61**	-2.40	-2.62
AC12	allamcin	**-4.66**	-1.76	-3.23
AC13	benzoic acid	**-5.29**	-4.10	-3.39
AC14	beta amyrin	-1.84	-1.96	**-2.80**
AC15	beta-Larabinopyranoside-methyl, 3-O-methyl-d-glucose, (Methyl beta-L-arabinopyranoside)	**-5.88**	-4.56	-4.36
AC16	beta-sitosterol	-2.02	**-2.26**	-1.96
AC17	cis, cis, cis-7,10,13-hexadecatrienal	**-5.95**	0.036	-2.59
AC18	D-glucopyranoside	**-6.51**	-4.23	-5.30
AC19	dodecanoic acid,(Lauric acid)	**-5.14**	-1.30	-3.12
AC20	glabiridin	**-6.24**	-1.49	-3.84
AC21	hexanoic acid(palmitic acid)	**-6.19**	-0.11	-2.41
AC22	isoplumericine	**-4.87**	-2.52	-3.57
AC23	kaempferol	-5.35	-3.47	**-5.63**
AC24	lupeol	**-4.25**	-0.43	**-**1.59

Compounds code	Compounds name	Docking score		
		PPAR-γ	GLP-1	DPP-4
AC25	naringenin	**-1.94**	-1.41	-1.68
AC26	nondecanoic acid	**-6.11**	-0.37	-1.91
AC27	octadecanoic acid (stearic acid)	**-7.12**	-2.22	-2.30
AC28	octanoic acid	-4.83	**-5.06**	-1.62
AC29	oleic acid	**-6.62**	-0.72	-2.47
AC30	pentadecanoic acid	**-5.92**	-1.01	-2.90
AC31	phytol	**-7.13**	-0.04	-2.09
AC32	plumericine	**-4.87**	-2.52	-3.57
AC33	plumeride coumerate	-1.26	-2.68	**-6.93**
AC34	quercetin	**-6.21**	-3.69	-4.93
AC35	squalene	**-7.02**	-0.77	-4.10
AC36	tetradecanoic acid (Myristic acid)	**-5.69**	-2.64	-3.08
AC37	thymine	**-6.18**	-3.78	-5.13
AC38	ursolic acid	-1.96	**-2.09**	-1.36
AC39	vitamin E	**-7.02**	-1.75	-2.81
	Alogliptin	-5.13	-2.83	**-9.02**
	Rosiglitazone	**-7.66**	-1.68	-3.98

The 2D diagram displayed interactions between compounds and PPARγ binding sites (Figs. 3 and 4). The interactions include hydrogen bonds, hydrophobic and electrostatic interaction, which play a significant role in the stability of receptor-ligand complexes. Among all of the interactions, hydrogen bond interactions are considered a more important criterion to evaluate the binding affinity and stable conformations. Compound **AC2** (1-deoxy-d-mannitol) and compound **AC31** (Phytol) exhibit the highest binding affinity for PPARγ in terms of docking score of -7.39 kcal/mol and − 7.13 kcal/mol. Compound **AC2** interacts with the PPARγ proteins through the formation of 7 hydrogen bonds with the amino acid residues Phe282, His449, Tyr327, His323 and Ser289. The residues involved in hydrophobic interactions are Leu469, Cys285, Phe282, Leu453, Phe363, Leu330, Tyr473, Ile326, Tyr327 and Leu465. Compound **AC31** forms two hydrogen bonds with His323 and Tyr473 amino acid residues. Rosiglitazone was considered as a reference drug for the comparison of the docked phytoconstituents with the PPARγ protein. The 2D and 3D protein-ligand contacts of the rosiglitazone are given in the Fig. 5. Reference

compound rosiglitazone forms two hydrogen bond with Hie323 and Ser289 residues while residues Ile326, Cys285, Phe282, Ile281, Tyr473, Phe363, Leu330 and Met364 contributes to the formation of hydrophobic interactions. Therefore, we concluded that the binding pocket occupied by **AC31** and **AC2** was identical to that of the original co-crystallized ligand rosiglitazone. The H-bond interaction was observed based on the ketone group of thiazolidinedione ring between the rosiglitazone and the key residues of the pockets such as Ser289 and Hie323. Above all, the compound **AC2** had more interactions than the reference rosiglitazone, which resulted in a much better binding affinity.

3.3 ADMET calculations

We predicted ADMET properties of 05 molecules which were selected from the docking result for further analysis. The results of the selected parameters of ADMET are represented in Table 3. It indicated the compound AC2, AC31 and AC35 shows no violation for toxicity such as hepatotoxicity, skin sensitization and AMES toxicity. Only compound AC2 exhibit less intestinal absorption among all compounds which can be increases by forming a formulation. In the addition, the all compounds also fell in the 99% BBB ellipse, indicating that these compounds can penetrate BBB.

Table 3
ADMET profiles of the selected phytoconstituents with reference compounds

Parameters	AC2	AC31	AC3	AC35	AC27	Rosiglitazone
Intestinal absorption (human)	25.313%	91.162%	97.063%	91.888%	91.317%	95.871%
Skin Permeability	-4.362	-2.569	-2.452	-2.773	-2.726	-3.452
BBB permeability	-1.475	0.811	0.517	1.008	-0.195	-0.618
CNS permeability	-5.8	-1.566	-1.288	-0.972	-1.707	-2.788
Total Clearance	0.892	1.686	0.151	1.791	1.832	0.106
Hepatotoxicity	**No**	**No**	No	**No**	No	Yes
Skin Sensitisation	**No**	**No**	Yes	**No**	Yes	No
AMES toxicity	**No**	**No**	Yes	**No**	No	No

3.4 Molecular dynamics simulation

100 ns MD simulations were performed to evaluate the steady nature and conformations stability of the receptor-ligands complex (receptors: PPARα/γ; ligands: AC2 and AC31). It simulated a real physiological environment with temperature, pressure and water molecules. The analyzed results are displayed in Fig. 6–9. As shown in Fig. 6, the quantitative parameter root-mean-square deviation (RMSD) was used to assess the structural stability of receptor–ligand complex. For the PPARγ-AC2 complex, the RMSD tended to the equilibrium after the 25 ns simulations. The RMSD stable range of the PPARγ-AC2 complex was 0.8–2.8 Å (about 1.75 Å), which was distinctly lower than that of the PPARγ-AC31 complex (2.4 Å) in

Fig. 6 (B). For PPARγ-AC31 complex the equilibrium of the complex on the RMSD was reached after 40 ns simulation.

The root-mean-square fluctuation (RMSF) diagrams of in the MD trajectories were calculated in Fig. 7. Additionally, the *N*- and *C*-terminals of the protein vary more than any other region, according to the RMSF plot. Because they are often more rigid than the protein's unstructured portion, parts of secondary structure like alpha helices and beta strands change less than loop sections. The RMSF of the PPARγ-AC2 complex was found to be 1.4 Å whereas the PPARγ-AC31 complex shows an RMSF of 1.8 Å. In both complexes, the fluctuation tendency is consistent. The Protein-ligand interactions have been monitored all over the simulation in 100 ns in Fig. 8. These interactions were divided into hydrogen bond interaction, hydrophobic interaction, and ionic and water bridges. Values over 1.0 are possible, because multiple interactions of the same subtype with the ligand might be made (Yadava, Gupta, et al., 2015).

As can be seen in Fig. 8, the contacts of PPARγ-AC2 complex and PPARγ-AC31 complex, included hydrogen bond interaction, hydrophobic interaction and water bridges. The key amino acid residues including Phe282, Leu330, Phe363, Met364, His323, Ile326, Tyr327, Tyr473 and His449 all formed hydrogen bond interactions. Leu469, Cys285, Phe282, Leu453, Phe363, Leu330, Tyr473, Ile326, Tyr327 and Leu465 amino acid residues forms hydrophobic interactions. These results are found consistent with the molecular docking outcomes. From Fig. 9, for the PPARγ-AC2 complex, the values of ligand RMSD (average = 1.6 Å), RoG (average = 2.55 Å), and PSA (average = 195 $Å^2$) were calculated. And for the PPARγ-AC31 complex, ligand RMSD, RoG and PSA were found to be 2.0 Å, 5.4 Å and 50 $Å^2$, respectively. Based on these findings, it may be concluded that the ligand was bound to the protein during the simulation since none of the complexes conformations were unstable and no unfolding or folding took place.

4. Conclusion

The results of the present investigation suggest that *Allamanda cathertica* exerts antidiabetic effects through the activation of the PPARγ receptor. The bioactive phytochemicals of the *Allamanda cathertica* showed excellent bioactivity for GPCR and nuclear receptors. The majority of the phytoconstituents show considerable biological activity based on bioactivity score prediction. Further, molecular docking studies proved that most of the phytoconstituents show excellent binding with the PPARγ receptor in terms of docking score. All the constituents bind with the protein in a similar way as the reference compound rosiglitazone interacts with PPARγ receptor. Compound **AC2** interacts with the PPARγ proteins through the formation of 7 hydrogen bonds with the residues Phe282, His449, Tyr327, His323 and Ser289 while compound **AC31** forms two hydrogen bonds with His323 and Tyr473 amino acid residues. Hydrophobic contacts were also seen between the receptor and ligand. Docking suggests that the binding of ligands with PPARγ governed by the hydrogen bond and hydrophobic interactions. The stability of the docked compounds was evaluated through molecular dynamics simulations. Results revealed that both ligands cope well with the target protein and docked complexes were stabilized by majorly hydrogen bond and hydrophobic interactions. Based on these investigations, further studies are

required to evaluate *in-vitro* and *in-vivo* techniques. Conclusively, the findings of this research could help researchers who are struggling continuously for the development of novel and effective drugs from natural products. The observed phytochemical diabetic potential of this plant indicated that it might be valuable for further studies of bioactive compounds.

Declarations

Acknowledgments - The authors are grateful to the scientific community.

Compliance with Ethical Standards

Conflicts of interest: The authors declare no conflict of interest associated with this work.

Ethical Approval: The authors did not need any ethical approval for the manuscript.

Funding: The authors did not receive funding support from any organization.

Author Contribution

Conceptualization: Santosh Kumar Rath; Methodology: Mrs. Ritu Tomar, Dr. Santosh Kumar Rath, Dr. Shashank Shekher Mishra; Formal analysis and investigation: Dr. Jagannath Sahoo; Software: Dr. Shashank Shekher Mishra; Writing - original draft preparation: Mrs. Ritu Tomar, Dr. Santosh Kumar Rath; Writing - review and editing: Dr. Santosh Kumar Rath, Dr. Jagannath Sahoo, Supervision: Santosh Kumar Rath.

References

1. Bermúdez, V., Finol, F., Parra, N., Parra, M., Pérez, A., Peñaranda, L., Vílchez, D., Rojas, J., Arráiz, N., & Velasco, M. (2010). PPAR-γ Agonists and Their Role in Type 2 Diabetes Mellitus Management. American Journal of Therapeutics, 17(3), 274–283. https://doi.org/10.1097/mjt.0b013e3181c08081.
2. Bonomini, T. J., Holzmann, I., Thiesen, L. C., Fratoni, E., Muller, A. F. F., Lucinda-Silva, R. M., Yunes, R. A., Malheiros, A., Gonçalves, A. E., Dalmagro, A. P., da Silva, K. A. B. S., de Souza, M. M., & Santin, J. R. (2017). Neuropharmacological and acute toxicological evaluation of ethanolic extract of Allamanda cathartica L. flowers and plumieride. Regulatory Toxicology and Pharmacology, 91, 9–19. https://doi.org/10.1016/j.yrtph.2017.10.005.
3. Bruning, J. B., Chalmers, M. J., Prasad, S., Busby, S. A., Kamenecka, T. M., He, Y., Nettles, K. W., & Griffin, P. R. (2007). Partial Agonists Activate PPARγ Using a Helix 12 Independent Mechanism. Structure, 15(10), 1258–1271. https://doi.org/10.1016/j.str.2007.07.014.
4. Cheng, X., Wang, X.-J., Zhang, J., Wang, S.-Q., Xu, W.-R., & Wang, R.-L. (2014). Identification of novel multitargeted PPARα/γ/δ pan agonists by core hopping of

rosiglitazone. Drug Design, Development and Therapy, 2255. https://doi.org/10.2147/dddt.s70383.

5. Cronet, P., Petersen, J. F. W., Folmer, R., Blomberg, N., Sjöblom, K., Karlsson, U., Lindstedt, E.-L., & Bamberg, K. (2001). Structure of the PPARα and -γ Ligand Binding Domain in Complex with AZ 242; Ligand Selectivity and Agonist Activation in the PPAR Family. Structure, 9(8), 699–706. https://doi.org/10.1016/s0969-2126(01)00634-7.
6. Dokhe, P., Girme, S., Barawant, M. M., & Abdi, G. (2023). Biochemical, Phytochemical Screening and Pharmacological Potential of Allamanda blanchetii (Purple Allamanda). INTERNATIONAL JOURNAL OF PLANT AND ENVIRONMENT, 9(01), 89–92. https://doi.org/10.18811/ijpen.v9i01.15.
7. Engwa, G., Nwalo, F., Chiezey, V., Unachukwu, M., Ojo, O., & Ubi, B. (2018). Assessment of the Pro12Ala Polymorphism in the PPAR-γ2 Gene among Type 2 Diabetes Patients in a Nigerian Population. Journal of Clinical Medicine, 7(4), 69. https://doi.org/10.3390/jcm7040069.
8. Feng, X.-Y., Ding, T.-T., Liu, Y.-Y., Xu, W.-R., & Cheng, X.-C. (2020). In-silico identification of peroxisome proliferator-activated receptor (PPAR)α/γ agonists from Ligand Expo Components database. Journal of Biomolecular Structure and Dynamics, 39(5), 1853–1864. https://doi.org/10.1080/07391102.2020.1745279.
9. Hameed, A., Nawaz, G., & Gulzar, T. (2014). Chemical composition, antioxidant activities and protein profiling of different parts ofAllamanda cathartica. Natural Product Research, 28(22), 2066–2071. https://doi.org/10.1080/14786419.2014.923997.
10. Hong, O.-Y., Youn, H. J., Jang, H.-Y., Jung, S. H., Noh, E.-M., Chae, H. S., Jeong, Y.-J., Kim, W., Kim, C.-H., & Kim, J.-S. (2018). Troglitazone Inhibits Matrix Metalloproteinase-9 Expression and Invasion of Breast Cancer Cell through a Peroxisome Proliferator-Activated Receptor γ-Dependent Mechanism. Journal of Breast Cancer, 21(1), 28. https://doi.org/10.4048/jbc.2018.21.1.28.
11. Jain, R. K., & Laiteerapong, N. (2015). Strategies for Improving Cardiovascular Health in Women With Diabetes Mellitus: a Review of the Evidence. Current Diabetes Reports, 15(11). https://doi.org/10.1007/s11892-015-0665-7.
12. Jia, W.-Q., Jing, Z., Liu, X., Feng, X.-Y., Liu, Y.-Y., Wang, S.-Q., Xu, W.-R., Liu, J.-W., & Cheng, X.-C. (2017). Virtual identification of novel PPARα/γ dual agonists by scaffold hopping of saroglitazar. Journal of Biomolecular Structure and Dynamics, 36(13), 3496–3512. https://doi.org/10.1080/07391102.2017.1392363.
13. Kurtzhals, l., nørgaard, s., ronneby, h., secher, a. L., tabor, a., mcintyre, h. D., damm, p., & mathiesen, e. R. (2018). The Impact of Restricted Gestational Weight Gain on Fetal Growth during Dietary Treatment in Women with Gestational Diabetes Mellitus. Diabetes, 67(Supplement_1). https://doi.org/10.2337/db18-689-p.
14. Liu, X., Jing, Z., Jia, W.-Q., Wang, S.-Q., Ma, Y., Xu, W.-R., Liu, J.-W., & Cheng, X.-C. (2017). Identification of novel PPARα/γ dual agonists by virtual screening, ADMET prediction and molecular dynamics simulations. Journal of Biomolecular Structure and Dynamics, 36(11), 2988–3002. https://doi.org/10.1080/07391102.2017.1373706.

15. McIntyre, H. D., Catalano, P., Zhang, C., Desoye, G., Mathiesen, E. R., & Damm, P. (2019). Gestational diabetes mellitus. Nature Reviews Disease Primers, 5(1). https://doi.org/10.1038/s41572-019-0098-8.
16. Mishra, S. S., Kumar, N., Singh, H. P., Ranjan, S., & Sharma, C. S. (2018). In silico Pharmacokinetic, Bioactivity and Toxicity study of Some Selected Anti-asthmatic Agents. International Journal of Pharmaceutical Sciences and Drug Research, 10(4). https://doi.org/10.25004/ijpsdr.2018.100411.
17. Mudaliar, S., & Henry, R. R. (2004). Thiazolidinediones as PPAR Agonists. International Textbook of Diabetes Mellitus. Portico. https://doi.org/10.1002/0470862092.d0611.
18. Nolte, R. T., Wisely, G. B., Westin, S., Cobb, J. E., Lambert, M. H., Kurokawa, R., Rosenfeld, M. G., Willson, T. M., Glass, C. K., & Milburn, M. V. (1998). Ligand binding and co-activator assembly of the peroxisome proliferator-activated receptor-γ. Nature, 395(6698), 137–143. https://doi.org/10.1038/25931.
19. Petricevich, V., & Abarca-Vargas, R. (2019). Allamanda cathartica: A Review of the Phytochemistry, Pharmacology, Toxicology, and Biotechnology. Molecules, 24(7), 1238. https://doi.org/10.3390/molecules24071238.
20. Pires, D. E. V., Blundell, T. L., & Ascher, D. B. (2015). pkCSM: Predicting Small-Molecule Pharmacokinetic and Toxicity Properties Using Graph-Based Signatures. Journal of Medicinal Chemistry, 58(9), 4066–4072. https://doi.org/10.1021/acs.jmedchem.5b00104.
21. Prabhadevi, V., Sahaya, S. S., Johnson, M., Venkatramani, B., & Janakiraman, N. (2012). Phytochemical studies on Allamanda cathartica L. using GC–MS. Asian Pacific Journal of Tropical Biomedicine, 2(2), S550–S554. https://doi.org/10.1016/s2221-1691(12)60272-x.
22. Rodrigues, D., Muller, A. F., Bonomini, T., Klein-Júnior, L., Lucinda-Silva, R., & Malheiros, A. (2020). CHEMICAL VARIABILITY OF Allamanda cathartica L. FLOWERS ASSESSED BY MULTIVARIATE DATA ANALYSIS. Química Nova. https://doi.org/10.21577/0100-4042.20170467.
23. Sharma, C. S., Mishra, S., Singh, H., & Kumar, N. (2016). In silico ADME and Toxicity Study of Some Selected Antineoplastic Drugs. International Journal of Pharmaceutical Sciences and Drug Research, 8(01). https://doi.org/10.25004/ijpsdr.2016.080110.
24. Sharma, G., Kumar, N., Sharma, C. S., & Mishra, S. S. (2023). In silico guided screening of active components of C. lanceolata as 3-chymotrypsin-like protease inhibitors of novel coronavirus. 3 Biotech, 13(10). https://doi.org/10.1007/s13205-023-03745-2.
25. Shekhar Mishra, S., Sharma, C. S., Singh, H. P., Pandiya, H., & Kumar, N. (2016). In silico ADME, Bioactivity and Toxicity Parameters Calculation of Some Selected Anti-Tubercular Drugs. International Journal of Pharmaceutical and Phytopharmacological Research, 6(6), 77. https://doi.org/10.24896/eijppr.2016661.
26. Santosh K. Rath, S. Singh, S. Kumar, N. A. Wani, R. Rai, S. Koul, I.A. Khan & P.L. Sangwan, (2019). Synthesis of amides from (E)-3-(1-chloro-3, 4-dihydronaphthalen-2-yl) acrylic acid and substituted amino acid esters as NorA efflux pump inhibitors of Staphylococcus aureus. *Bioorganic & Medicinal Chemistry*, *27*(2), 343-353. https://doi.org/10.1016/j.bmc.2018.12.008

27. Shi, R., Zhao, L., & Qi, Y. (2018). The effect of fenofibrate on early retinal nerve fiber layer loss in type 2 diabetic patients: a case-control study. BMC Ophthalmology, 18(1). https://doi.org/10.1186/s12886-018-0769-3.
28. Unnikrishnan, R., Anjana, R. M., & Mohan, V. (2016). Diabetes mellitus and its complications in India. Nature Reviews Endocrinology, 12(6), 357–370. https://doi.org/10.1038/nrendo.2016.53.
29. V. Dwibedi, S.S. Mishra, N. George, M. Joshi, G. Kaur, M. Gupta, & S.K Rath, (2023). Purification of ursolic acid and β-sitosterol from endophytic *Alternaria alternata* for their alpha-amylase inhibitory activity. *Journal of Biomolecular Structure and Dynamics*, 1-12. https://doi.org/10.1080/07391102.2023.2236717
30. Yadava, U., Gupta, H., & Roychoudhury, M. (2014). Stabilization of Microtubules by Taxane Diterpenoids: Insight from Docking and MD simulations. Journal of Biological Physics, 41(2), 117–133. https://doi.org/10.1007/s10867-014-9369-5.
31. Yun, S.-H., Han, S.-H., & Park, J.-I. (2018). Peroxisome Proliferator-Activated Receptor γ and PGC-1α in Cancer: Dual Actions as Tumor Promoter and Suppressor. PPAR Research, 2018, 1–12. https://doi.org/10.1155/2018/6727421.

Figures

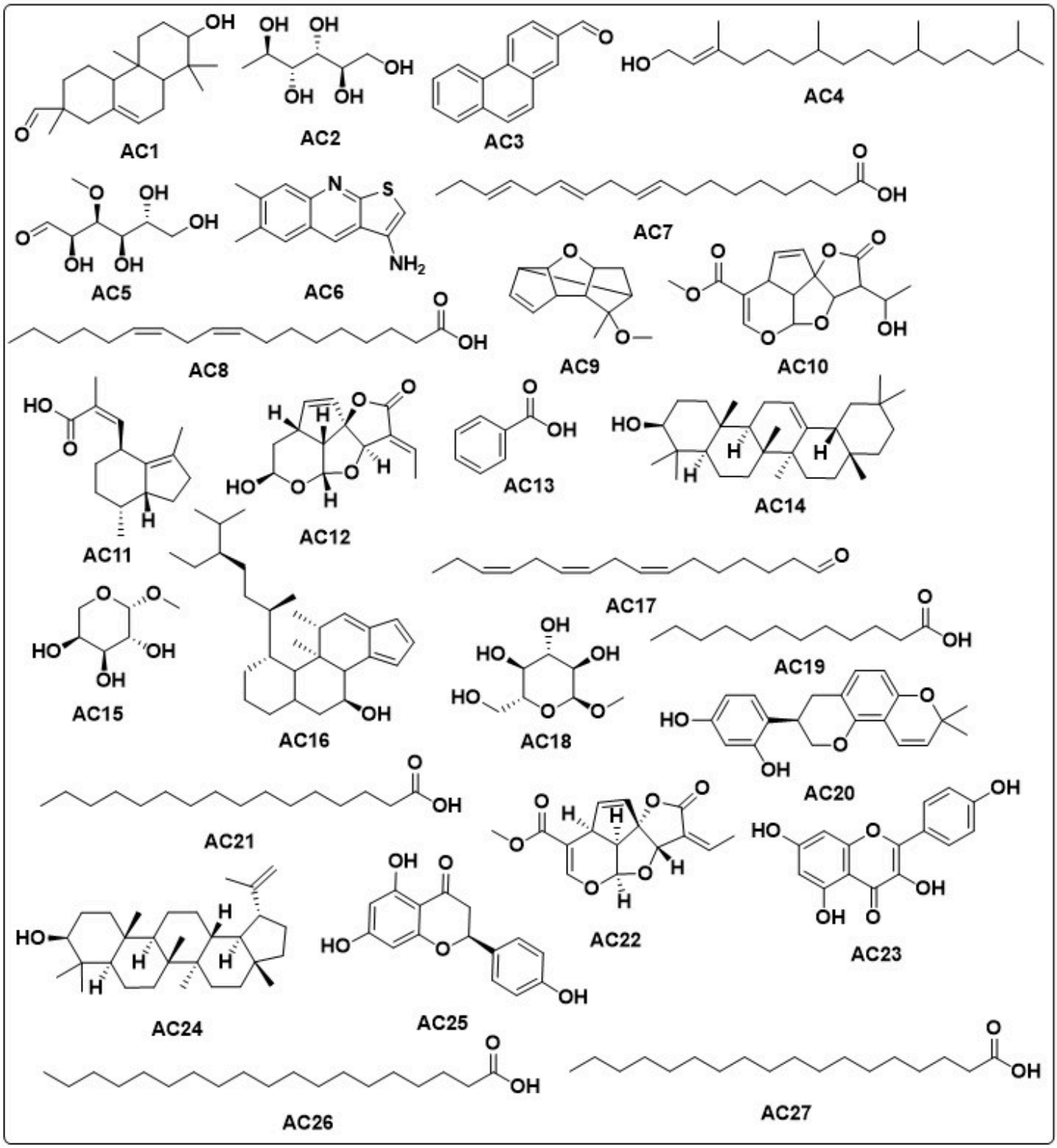

Figure 1

Chemical structures of the selected phytoconstituents (AC1 to AC27) of *Allamanda cathertica*.

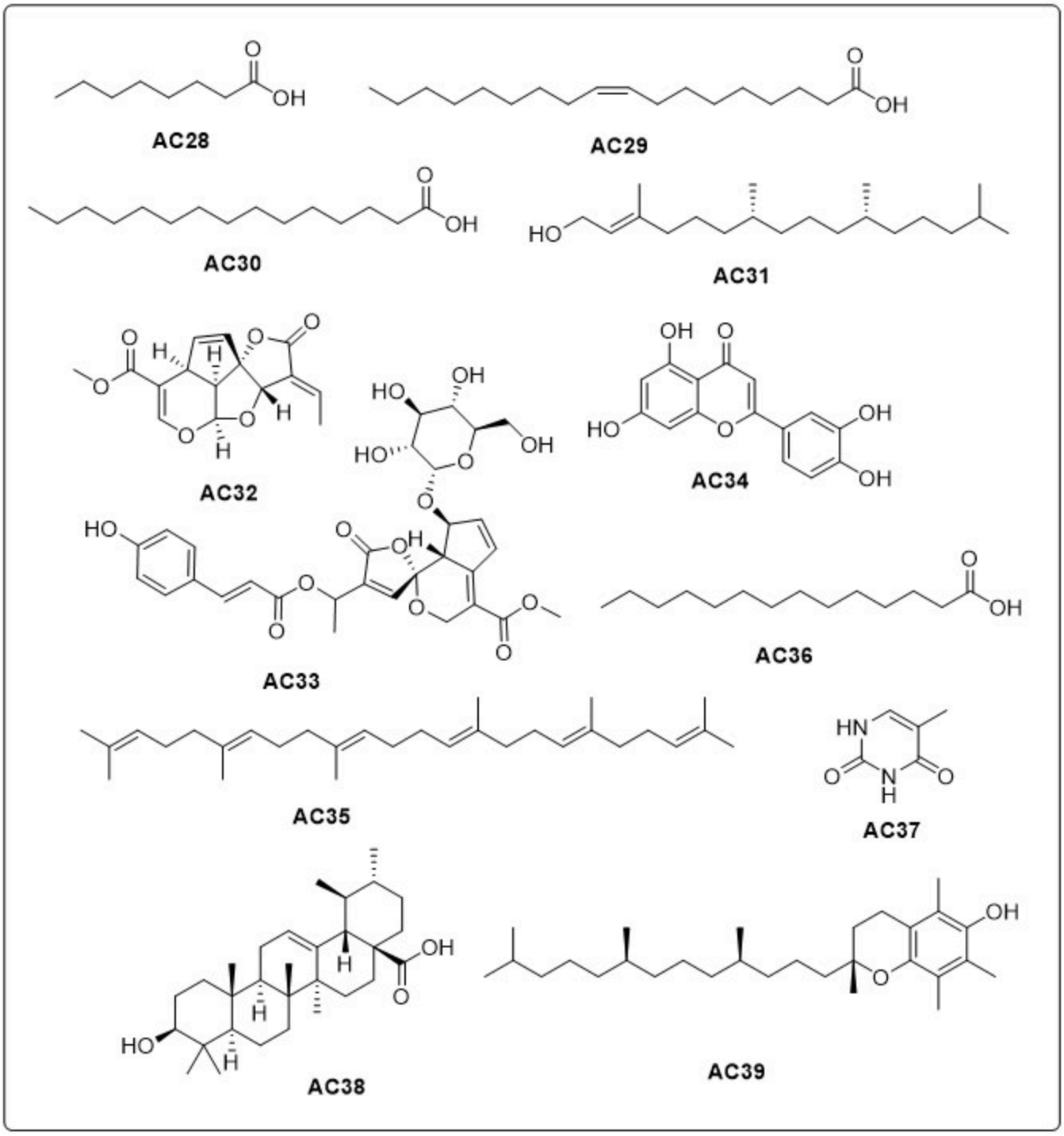

Figure 2

Chemical structures of the selected phytoconstituents (AC28 to AC39) of *Allamanda cathertica*.

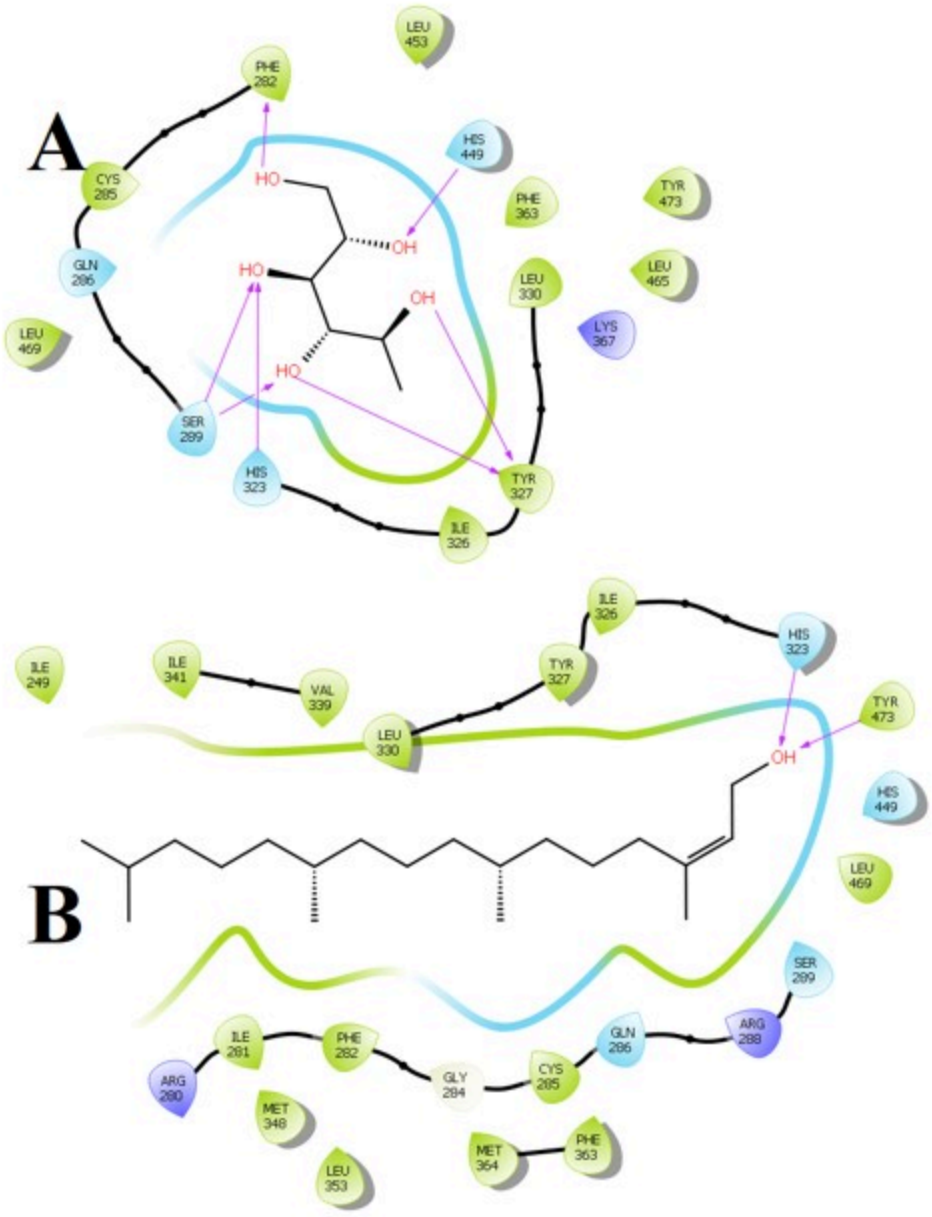

Figure 3

Two-dimensional (2D) PPARγ protein-ligand contacts of (A) Compound **AC2** and (B)**AC31.**

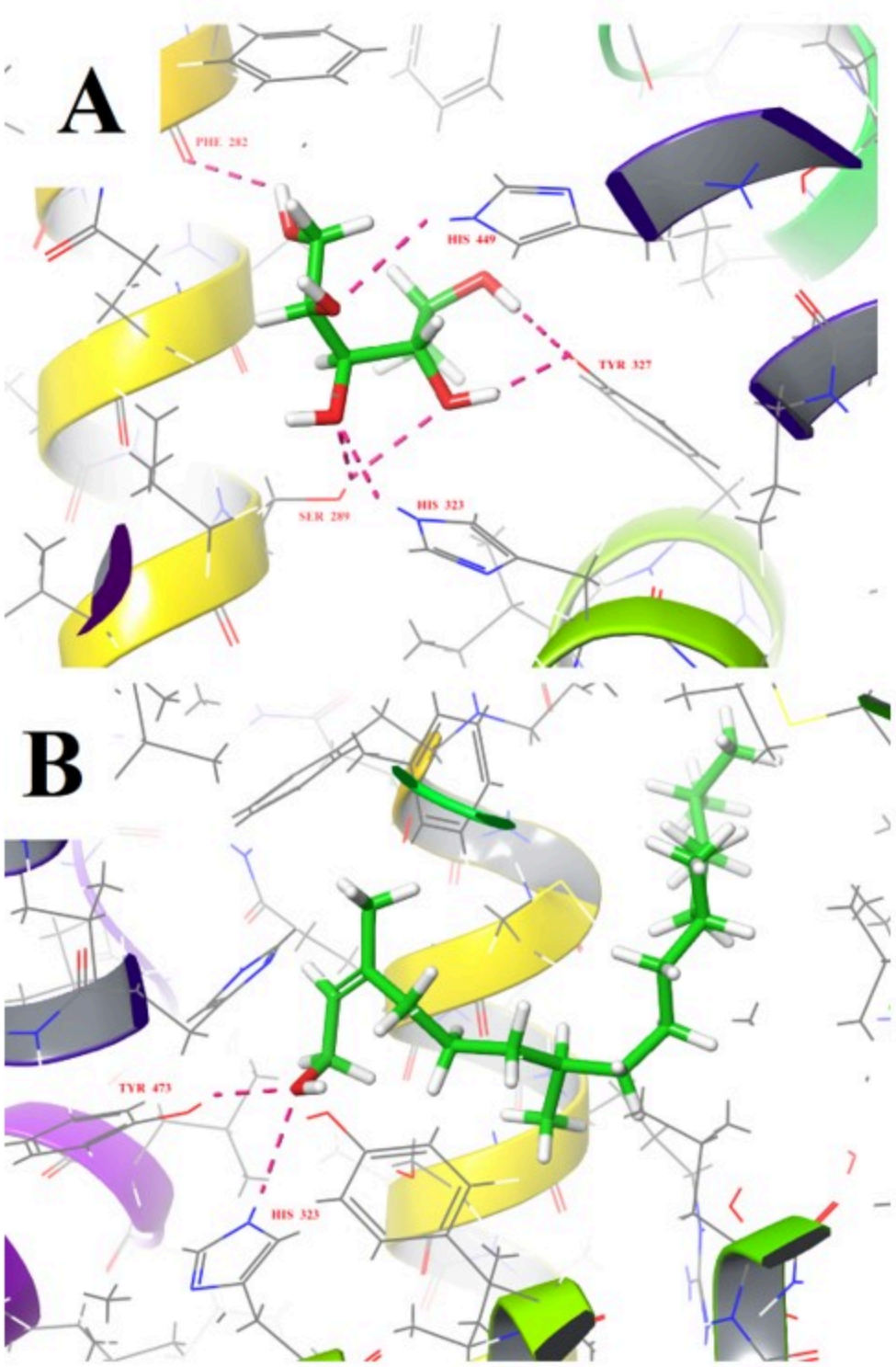

Figure 4

Binding conformations of the PPARγ protein-ligand (A) Compound **AC2** and (B)**AC31.**

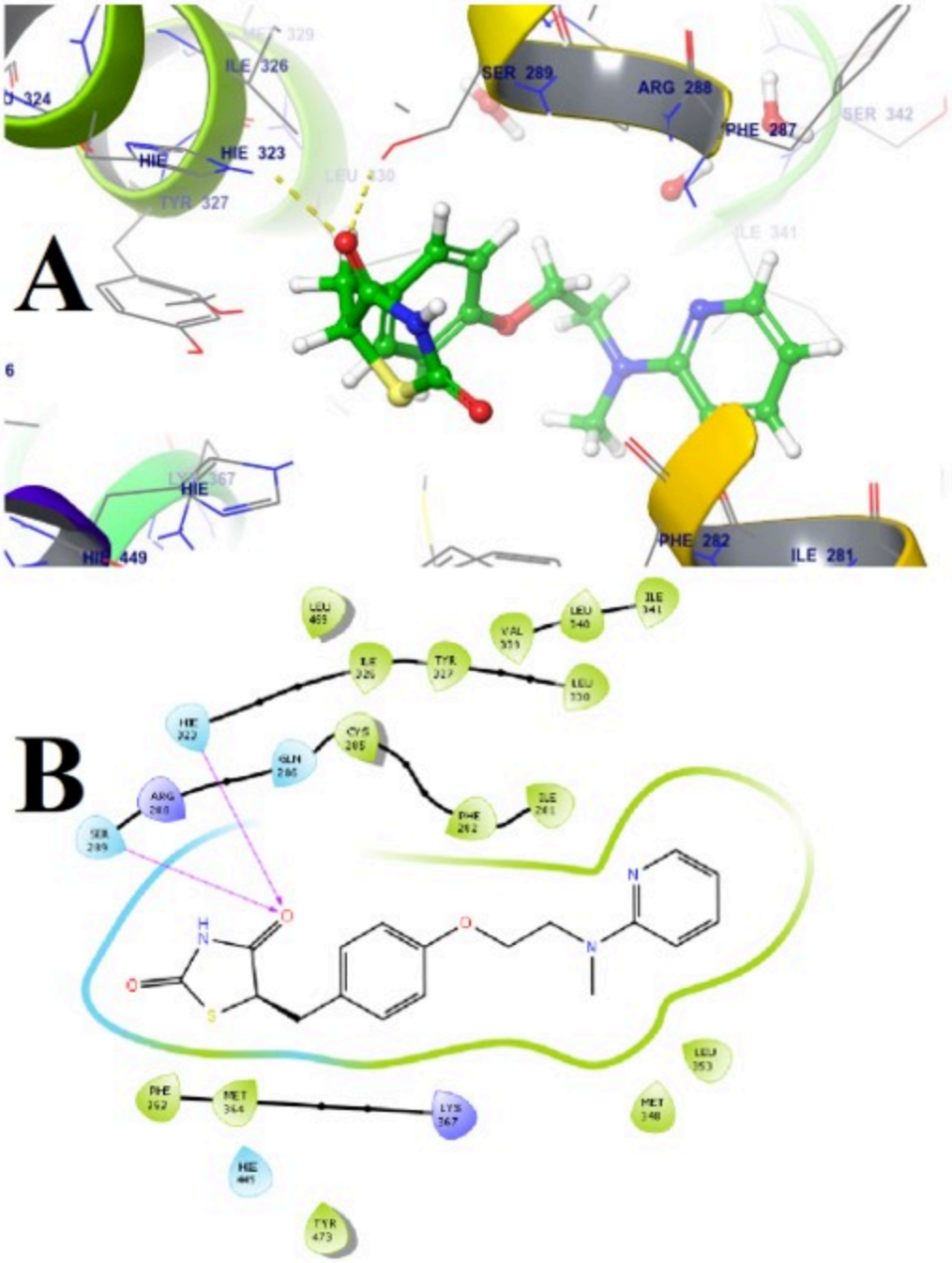

Figure 5

Binding mechanism of the Rosiglitazone with PPARγ protein (A) 3D diagram and (B) Protein-ligand contacts in 2D.

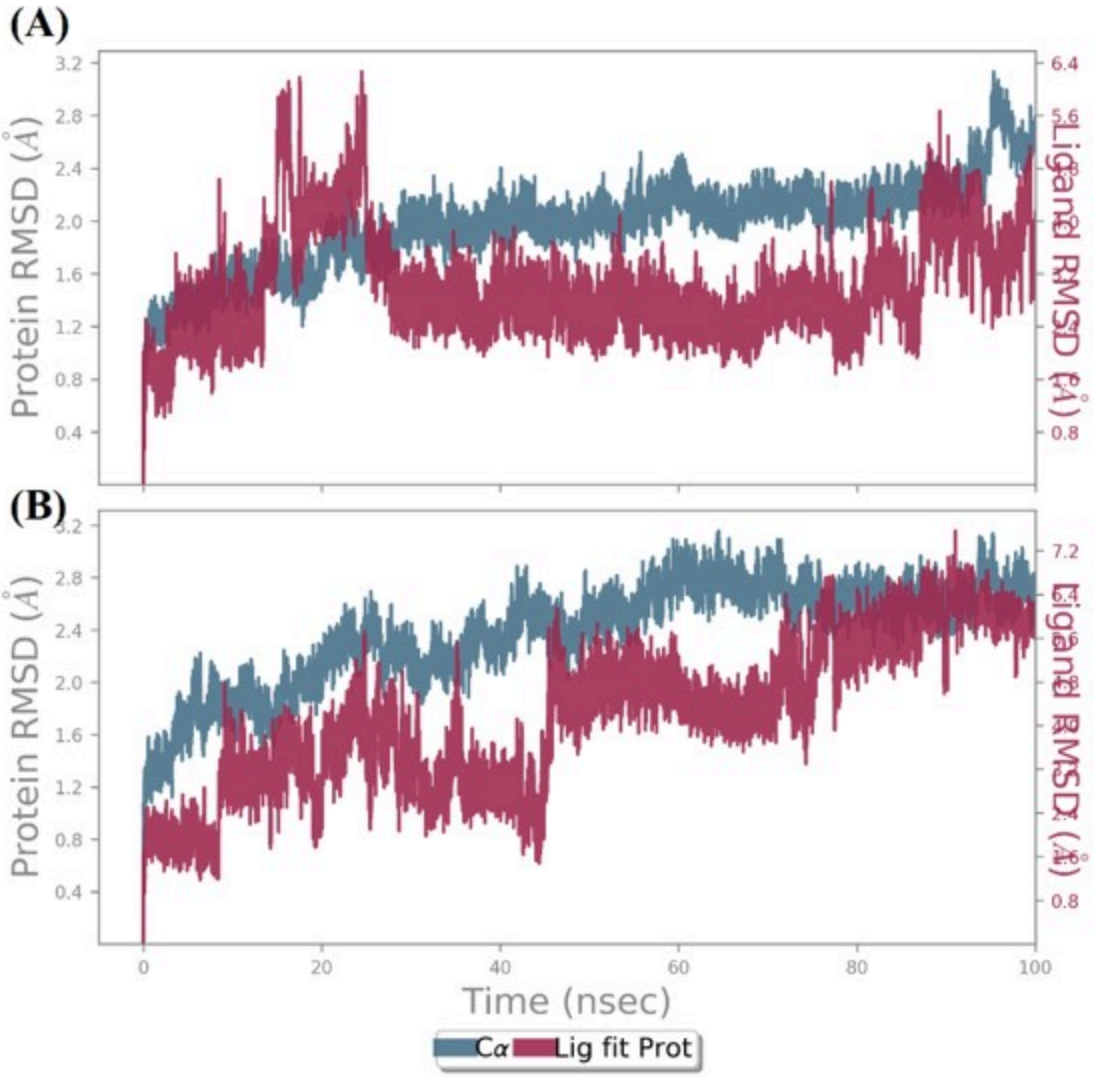

Figure 6

The RMSD plot for all backbone atoms for the (A) **PPARγ-AC2 complex** and (B) **PPARγ-AC31 complex.**

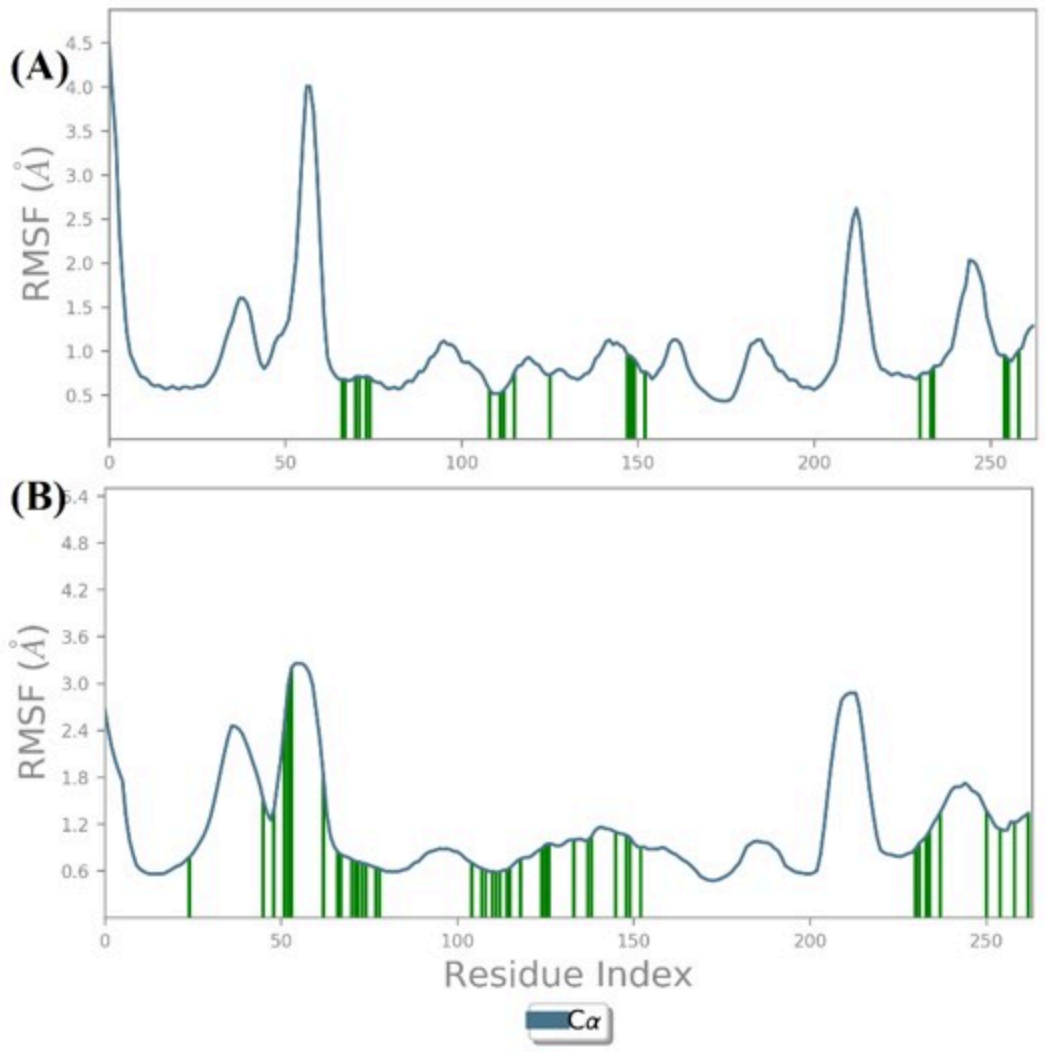

Figure 7

The RMSF plot of (A) **PPARγ-AC2 complex** and (B)**PPARγ-AC31 complex** over the entire simulations

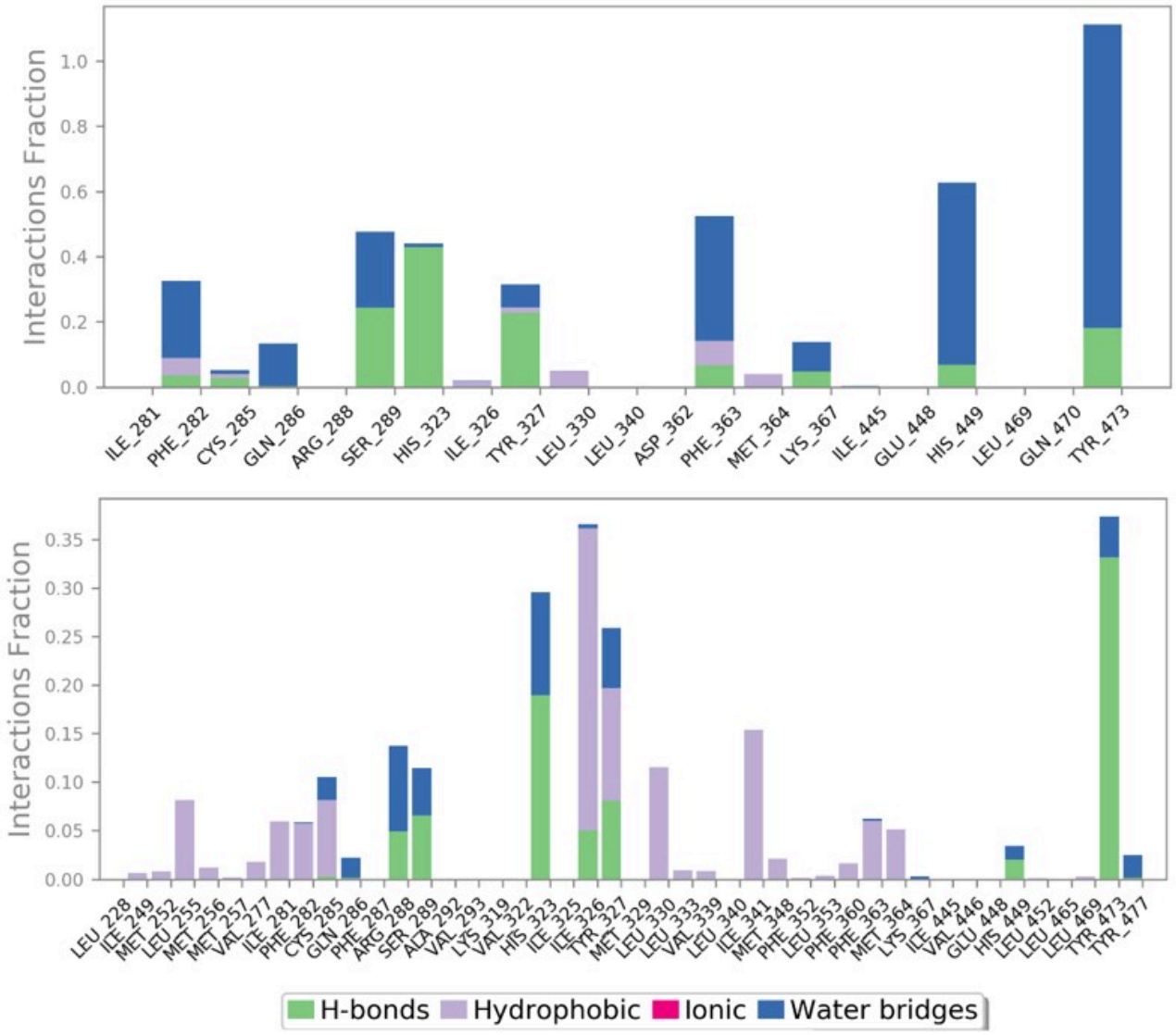

Figure 8

The bar diagrams of the protein-ligand contacts of (A) **PPARγ-AC2 complex** and (B) **PPARγ-AC31 complex.**

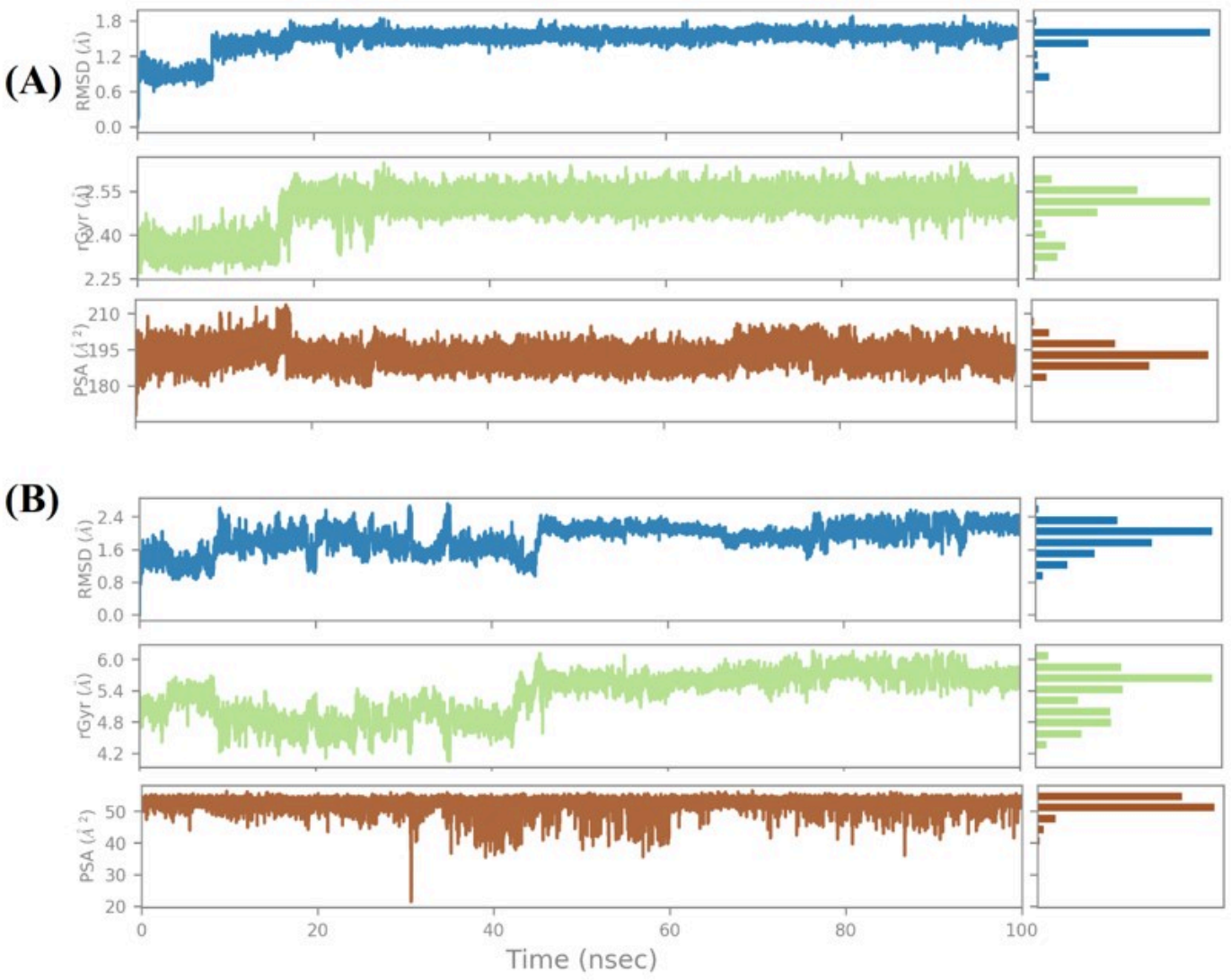

Figure 9

Ligand RMSD, Radius of gyration, PSA plot of (A) **PPARγ-AC2 complex** and (B)**PPARγ-AC31 complex.**

Supplementary Files

This is a list of supplementary files associated with this preprint. Click to download.

- GraphicalAbstract.docx